Ninth International Conference on Computational Fluid Dynamics (ICCFD9), Istanbul, Turkey, July 11-15, 2016

ICCFD9-xxxx

Simulations of Drop Impact on Hydrophobic Moving Walls

Hosein Heidarifatasmi, Özgür Ertunç

Department of Mechanical Engineering, Ozyegin University, Istanbul 34794, Turkey

Corresponding author: hosein.heidarifatasmi@ozu.edu.tr

Abstract: Numerical simulations of water drop impact onto a hydrophobic surface are carried out through usage of Eulerian multiphase model. Volume of fluid (VOF) model is used to capture the deformation of the water drop interface. RANS equations were solved by realizable $k-\epsilon$ turbulence model. Two and three dimensional simulations are conducted. Results of the simulations are compared with the published experimental data. Results for maximum drop spreading have errors below 10% compared to their experimental counterparts. It is shown that 2D simulations augments splitting of droplets due to entrapped bubbles upon impact while 3D simulations reproduce deposition observed in experiments, but partial rebound and split deposition phenomena can not be reproduced. The discrepancy between the experiments and 2D as well as 3D simulations are analyzed.

Keywords: Multiphase Flows, VOF Model, Drop Impacts, Moving Wall, Bubble Entrapment.

1 Introduction

Absorption of atmospheric gases (CO_2 or O_2) on the surface of the seas and oceans, spreading of organisms or micro-organisms like fungi and underwater rain noise are all examples of drop impacts in nature. But from first deliberate observations of drop impacts by a student [1], nowadays they have contributed into wide variety of industrial applications such as spray cooling, spray coating, ink-jet printing, internal combustion engines and erosion prevention in turbine blades. Impact of drops on dry solid surfaces, thin pre-existed liquid films and liquid pools are different modes of drop impacts [2]. Among them, impact of drops on solid surfaces is more relevant to the present work. Experimental studies on this subject have been done by many researchers [3, 4, 5, 6, 7, 8]. In terms of outcomes, considering solid dry surfaces, six disparate outcomes in consequence of drop impact is achieved as demonstrated by [6]. The drop might deposit if inertia is weak, undergo either prompt splash (for rough surfaces) or corona splash if inertial forces are prevailing over the surface tension, bounce off the surface in either partial rebound or total rebound mode. Some smaller drops originated from the mother drop might be left behind by the receding lamella which is called receding break up. Rioboo et al. (2002) [7] explained the effect of velocity, diameter, viscosity and surface tension of the drop, wettability and roughness on step by step evolution of the drop with time in kinematic, spreading and relaxation phases. An argument on appropriate impact factor $P = We/Re^{\frac{2}{5}}$ or $We/Re^{\frac{4}{5}}$ which shows the extent of importance of viscous and capillary forces compared to inertia in an impact scenario, is discussed in [8]. For more information on history of studies on drop impacts, we encourage the reader to take a look at [9, 10].

Studies of drop impacts on stationary solid surfaces would give us insights about the fundamental phenamona happening during impact process, but in most practical applications in which drop impacts are involved, the surface is moving. However, drop impacts on moving surfaces were investigated by a few researchers [11, 12, 13, 14]. Partial rebound, deposition and split deposition (see Fig. 1) were the outcomes

of water drop impacts on a Teflon surface [12]. In Fig.1 it is seen that the partial rebound happens at low We_t values together with the relatively high We_n numbers. Less energetic impacts would end up with deposition on the surface while split deposition which is disintegration of the water drop into two smaller drops happens at high We_t numbers. Semi-empirical relations were devised to classify the outcomes in We_n and We_t domain. However, deviation from the experimental data in split deposition regime while $We_n < 40$ is quite clear which means the current method is not good at categorizing the physical observations.

Bird et al. (2009) [11] examined the splashing regime for impacts with tangential velocity created by either an inclined surface or a moving disk. What they observed is below the splashing threshold, at sufficiently high tangential velocities, the portion of the lamella which is spreading in the opposite direction of the moving surface can experience splashing while the other portion which moves in the same direction experiences only spreading. Similarly, above the splashing threshold, at sufficiently high tangential velocities, one can suppress the splashing in the portion of the lamella which moves in the same direction as the moving surface whereas amplifying the splashing on the other side.

Zen et al. (2010) [14] studied the drop impacts on inclined and moving surfaces. Due to the wettability of the ethanol on the silicon wafer surface rebound did not occur but instead they were able to characterize deposition and splashing phenomena. The normal component of the We number was used to distinguish different outcomes and yet it was confirmed that $We = 210$ is a good threshold for occurrence of splashing for all different inclination angles. They observed, an increase in inclination angle leads to wider range of asymmetric splashing region which means more inertial is needed to create a two-side splash. Impacts on horizontal moving surfaces were done and provoking effect of the moving surface below the splashing threshold and restraining effect of it above the threshold in creating the one-side splashes, were confirmed.

Fathi et al. (2010) [13] investigated the case of train of drops impacting on a moving surface where frequency of generated drops is another key parameter. The nature of their investigation dictates that not only the kinetic energy of each individual drop is important but rather the rate of energy is of desire. It was shown increase in frequency would lead to decrease in drop size, increase in drop impingement rate and has almost no effect on drop velocity and flow rate. Effects of impingement rate, volume of the spreading drop and surface velocity, were considered through using the linear deposition rate which was defined as the volume of the deposited fluid to the unit displacement of the moving surface. Intuitively, an increase in surface motion speed will decrease the linear deposition rate but change in frequency had almost no effect on the behavior of the linear deposition rate. They also reported generation of a periodic crown-like wave in the advancing liquid layer for high linear deposition rates in contrast to the low values.

Front tracking, level-set, VOF and lattice-Boltzmann methods are available numerical algorithms to deal with multiphase flows. Level-set methods are powerful tools for analyzing and tracking the interface for evolving topologies in time based on an Eulerian approach [15]. Numerical studies of drop impacts have been done by several researchers [16, 17, 18, 19]. Lunkad et al. (2007) [17] simulated the drop impacts on horizontal and inclined solid surfaces with VOF model for different wettability conditions. Their results were predicting good for non-wettable surfaces while they were not capturing physical phenomena for wettable surfaces. Bararnia et al. (2013) [16] were using lattice-Boltzmann method to perform the simulations of falling drops. Hence considering the effect of gravitational and surface forces using Eotvos number. They showed the rate of deformation has direct proportionality to Eotvos number. In other words, the more the Eotvos number, the more is the deformation. Tryggvason et al. (2001) [19] used a front tracking method to capture any change at the interface by taking the whole domain as one fluid with different physical properties and added the interfacial interactions between two phases with source terms in their equations. Effect of Re number on maximum spreading diameter of drop and We number on the time scales of reaching to maximum drop spreading and equilibrium conditions were investigated by [18]. It was stated that as We number increases the mentioned time scales increase and there is a threshold for Re number in which after that point there is no serious effect on maximum spreading diameter.

The effect of impact velocity of the drop on behavior of air entrapment is imperative. For low velocities of impacting drop, in case of drop impacts on liquid pools, the air film can be stretched in such a way so that the drop even does not touch the liquid pool hence bouncing off the surface of the liquid pool. In contrast, for high velocities, the air film is going to rupture and it is shown that the higher the impact velocity the thicker would be the thickness of air film at the instant of rupturing. Because of the excessive velocity the air does not have time to be squeezed between the drop and surface of the liquid pool, consequently ruptures at larger thicknesses [20]. The thickness of air film is in the range of 2-5 μm for drop impacts on solid

surfaces while it is 1-2.5 μm for drop impacts on liquid pools [21]. As the drop is traveling towards the solid surface, the air between the solid surface and drop is going to be pressurized and since the only side which is deformable is the drop side, it will flatten the bottom side of the drop causing the contact in a circular shape instead of a point [22]. This will cause bubble entrapment right at the center of the drop at early stages of impact.

2 Problem Statement

Simulations of drop impacts on a moving surface is considered in the present work. Simulations have been done in Star-CCM+ software which is a commercial CFD package. Results of our simulations are compared with experimental data of [12]. Water and air phases are defined in an Eulerian multiphase model and VOF method is used to construct the flow equations in order to capture the interface. VOF model assumes that all immiscible fluid phases inside a control volume share velocity, pressure and temperature fields. Hence, it uses the same mass, momentum and energy conservation equations just like the single phase flow conditions. That single phase fluid is in fact the fluid with physical properties of its constituent phases with respect to their volume fractions. Equations for obtaining physical properties of the single fluid in each control volume is written in the following section.

$$\rho = \sum_i \rho_i \alpha_i \tag{1}$$

$$\mu = \sum_i \mu_i \alpha_i \tag{2}$$

where $\alpha_i = \frac{V_i}{V}$ is the volume fraction and ρ_i and μ_i are the density and dynamic viscosity of the i^{th} phase. Integral form of continuity and momentum equations in which star-CCM+ solves, are as follows:

$$\frac{\partial}{\partial t}\int_V (\rho\chi)\, dV + \int_A \rho(\mathbf{V} - \mathbf{V}_g)\, dA = \int_V (s_u)\, dV \tag{3}$$

$$\frac{\partial}{\partial t}\int_V (\rho\chi\mathbf{V})\, dV + \int_A \rho\mathbf{V}\otimes(\mathbf{V} - \mathbf{V}_g)\, dA = -\int_A PI\cdot\, dA + \int_A T\cdot\, dA + \int_V (f_r + f_g + f_p + f_u + f_\omega + f_L)\, dV \tag{4}$$

Where $\chi, \mathbf{V}, \mathbf{V}_g, P, I$ and T are the fraction of volume not occupied by porous media, velocity, grid velocity, pressure, identity matrix and viscous stress tensor. Also $f_r, f_g, f_p, f_u, f_\omega$ and f_L represent body force terms related to rotation, buoyancy, porous media, user-defined body forces, vorticity confinement specific force and electromagnetic fields respectively. Usually an advection equation is solved for volume fraction to consider the motion of the interface, however, in STAR-CCM+ the integral form of this equation is as follows:

$$\frac{d}{dt}\int_V \alpha_i\, dV + \int_A \alpha_i(\mathbf{V} - \mathbf{V}_g)\, dA = \int_V \left(s_{\alpha_i} - \frac{\alpha_i}{\rho_i}\frac{D\rho_i}{Dt}\right) dV \tag{5}$$

where $\alpha_i, \mathbf{V}, \mathbf{V}_g$ and s_{α_i} are the volume fraction of phase i, velocity, grid velocity and sink or source of the i^{th} phase. Also note that $\frac{D\rho_i}{Dt}$ term is the material derivative which contains the temporal and directional derivatives of density of i^{th} phase.

The surface tension force is a tensile force tangential to the interface between present phases. In STAR-CCM+, it is modeled as a volumetric force using the continuum surface force (CSF) approach proposed by [23]. The magnitude of this force depends on the nature of the fluids involving in simulation and temperature. Following equations show the formulation of surface tension in our simulations.

$$f_\sigma = f_{\sigma,n} + f_{\sigma,t} \; where \; f_{\sigma,n} = \sigma\kappa\mathbf{n},\; f_{\sigma,t} = \frac{\partial\sigma}{\partial t}t \tag{6}$$

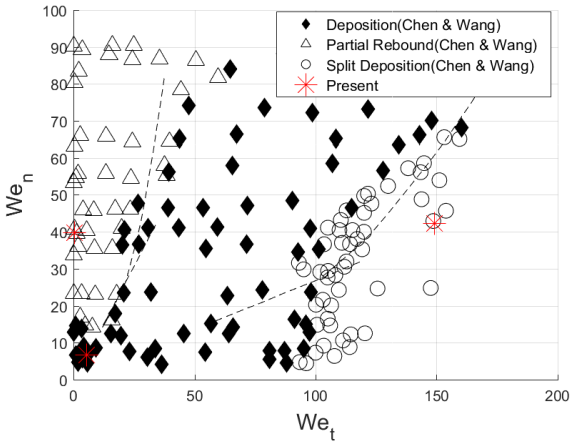

Figure 1: Outcomes of water drop impact on moving Teflon surface [12] and the simulations conducted in this work.

Table 1: Quantitative representation of selected data points and physical properties of water.

We_t	We_n	V_t (m/s)	V_n (m/s)	D (μm)	Outcome
0.3	39.8	0.2	2.4	500	Partial rebound
5.5	6.7	0.9	1	500	Deposition
149	42.3	4.7	2.5	500	Split deposition

Liquid	Density (kg/m^3)	Viscosity $(mPa.s)$	Surface tension (N/m)
Water	998	0.89	0.074

Where σ is the surface tension coefficient. f_σ is the surface tension force in which subscripts of n and t denote the normal and tangential components of this force respectively. $\mathbf{n}$ is the unit vector normal to the interface between phases and directing from liquid to gas phase. t is the unit vector in the tangential direction to the interface and κ is the mean curvature of the interface. CSF model uses the smooth field of the phase volume fraction α_i to calculate the normal vector to the interface. Equations regarding the calculation of normal vector to the interface and interface curvature are shown below.

$$\mathbf{n} = \nabla \alpha_i \tag{7}$$

$$\kappa = -\nabla \cdot \frac{\nabla \alpha_i}{|\nabla \alpha_i|} \tag{8}$$

Using an algorithm capable of altering the time step in favor of taking large time steps under the condition of keeping Courant number in $0.89 - 0.99$ range, helped us to use time steps dynamically and efficiently. Maximum and minimum allowable time steps were defined and the algorithm could use bigger time steps whenever it was possible.

Computational domain that we used for simulations was a rectangular cuboid with $9 \times 1 \times 2.5\ mm$ in size and it is sketched in Fig.2 along with boundary conditions and mesh. In all outer surfaces of this cuboid, the pressure outlet condition was selected except the one at the bottom which is the wall. The value of $0\ Pa$ was selected for the pressure outlet condition because it was set with respect to the reference pressure which was the atmospheric pressure. For the wall, no-slip condition was selected along with the static contact angle of water on Teflon which is 103°. Polyhedral mesh was selected for meshing the solution domain and near to 13 million cells were generated to spatially discretize the domain. Trajectory of the droplet while it is moving toward the surface and also a specific thickness from the wall were refined by using custom control mesh size option in STAR-CCM+. The closest distance from the wall in which we could resolve was $5\mu m$. Water drops were $500\mu m$ in diameter and with the mentioned resolution 100 cells were used across the diameter of the droplet. However, for 2D simulations there were almost 250000 cells present and a structured mesh was used. Droplet was defined by field function and using volume fraction variable. Three different impact scenarios were selected for simulations of drop impact on moving walls as shown in Fig.1 by red asterisks.

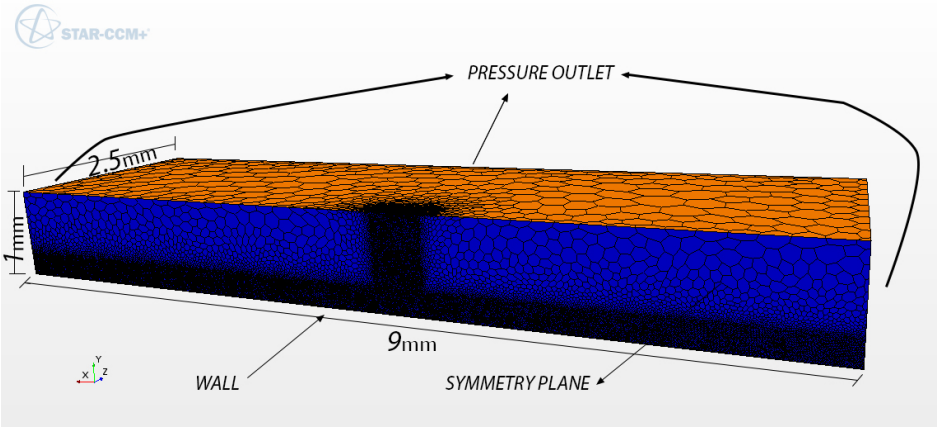

Figure 2: Computational domain, mesh and boundary conditions for the simulations of drop impact on moving walls.

3 Results and Discussion

3.1 Air entrapment

As the drop goes towards the solid wall, the air in between the drop and solid surface is going to be compressed and pressure rises (see Fig. 3). For the case of partial rebound ($V_t = 0.2\ m/s$, $V_n = 2.4\ m/s$) the gauge pressure of air right at the center of the droplet was about $7Pa$ when the distance between the drop and surface was $195\mu m$ whereas it increased to 50 Pa when the distance was about $50\mu m$. As an example, pressure field of the air phase is sketched in Fig. 4 where the distance between the drop and surface is $50\mu m$. Fig. 5 shows the pressure distribution at the moment of impact where pressure waves propagating inside the drop due to the impact, are visible.

3.2 Comparison of 2D and 3D simulations

In terms of outcomes, the results of 2D simulations are depicted in Fig. 6a, 6b, 6c.The first case ($We_t = 0.3, We_n = 39.8$) shows a condition in which the drop undergoes partial rebound in experiments while in our simulations it is splitting. As the drop is spreading over the surface, the thickness of the liquid film is decreasing and there would be more chances for the bubble to tear the liquid surface at the center of the film where it is located. By looking at states $t = 1, 1.7ms$, it is clear that the entrapped bubble helps to tear apart the drop at its center when we are at latest stages of spreading and beginning of receding. This behavior augments the split deposition in 2D simulations while it is not happening in 3D simulations at all (see Fig. 7). Because of the motion of the surface one portion of the drop which is moving in the same direction of the surface movement is going to spread more and the other portion which is moving in opposite direction is going to spread less. For small tangential velocities the spreading drop would look like a smoothed oval shape but as the velocity of the surface increases it will more look like a tear shape. Entrapped bubbles move towards the surface motion direction and cause partial rupture of drop at some points ($t = 0.6ms$). When the drop starts the receding phase, those areas will merge with each other as it favors the minimization of the contact surface because of surface tension force ($t = 1.4ms$) and finally escape from the liquid as the drop recoils ($t = 1.9ms$). The portion which was moving in the opposite direction of movement of surface will move in the same direction with respect to surface motion when receding starts. This is the reason why the drop tends to jump from its back side in our time evolution figure of drop. However, we got total rebound as the outcome of this scenario which is mainly due to the usage of static contact angle in our models. By looking at experimental outcomes of [12] one can clearly see that the contact angles are way different from the static one as we have dynamics of the triplet line. Generally, when the surface is pulling the liquid it favors the wettability and when they are in the opposite direction it tends to have high contact angles.

The second case ($We_n = 6.7, We_t = 5.5$) refers to the condition where deposition happens which means the drop hits the surface, spreads over the surface, recedes and finally after some oscillations it will deposit

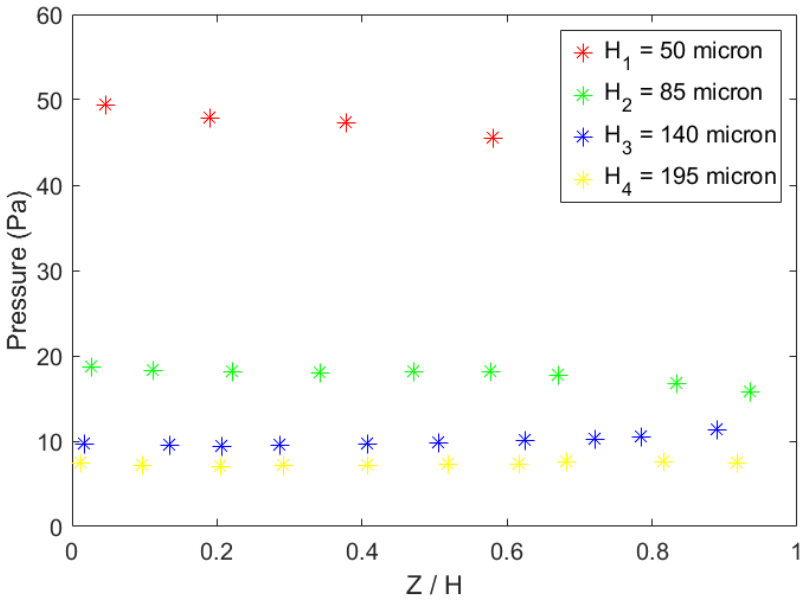

Figure 3: Pressure of the air film (gauge pressure with respect to ambient atmospheric pressure) between the droplet and solid surface as a function of non-dimensional height (Z/H). This simulation file corresponds to the 3D case of partial rebound ($We_t = 0.3, We_n = 39.8$)

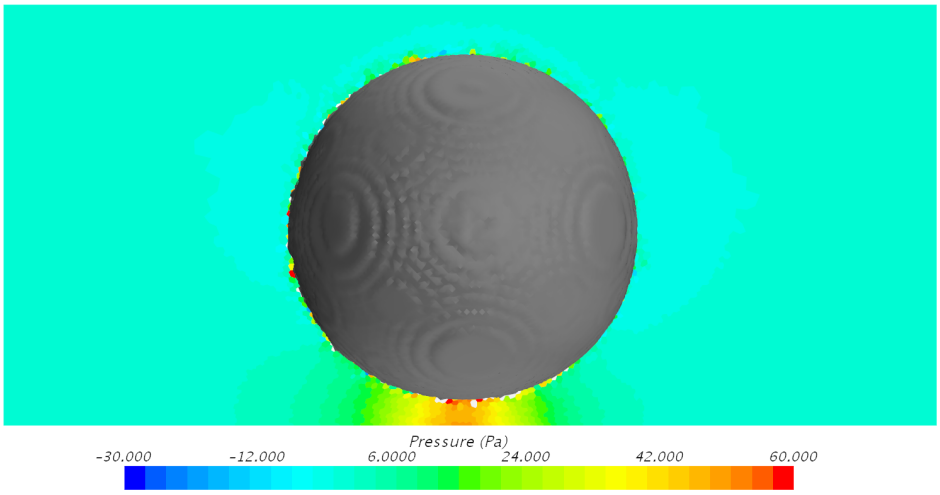

Figure 4: Pressure of the air film (gauge pressure with respect to ambient atmospheric pressure) between the droplet and solid surface (the distance is $50\mu m$). This simulation file corresponds to the 3D case of partial rebound ($We_t = 0.3, We_n = 39.8$)

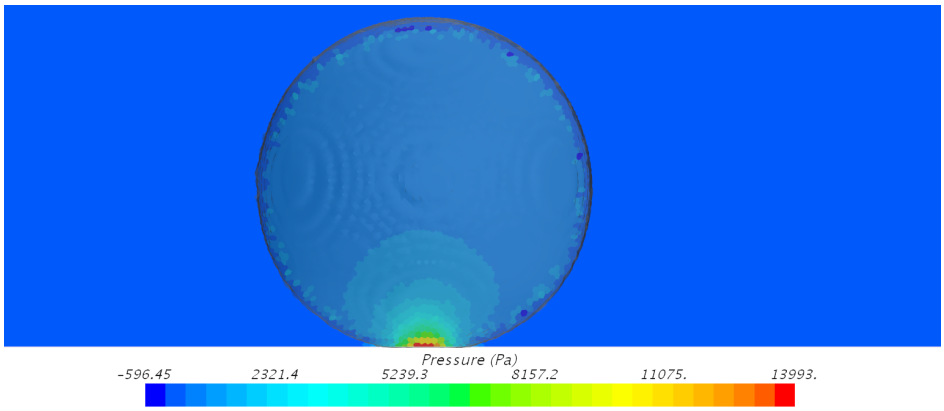

Figure 5: Pressure distribution (gauge pressure with respect to ambient atmospheric pressure) in solution domain right after impact. This simulation file corresponds to the 3D case of partial rebound ($We_t = 0.3, We_n = 39.8$)

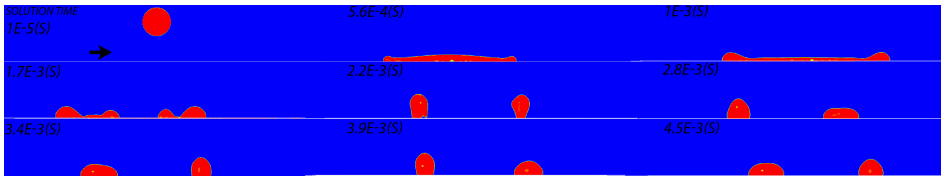

(a) Partial rebound

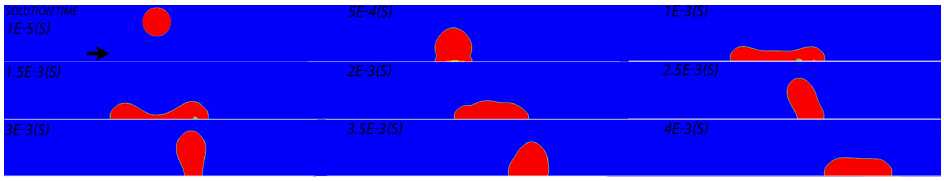

(b) Deposition

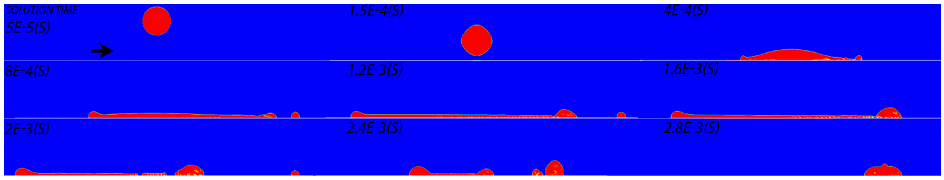

(c) Split deposition

Figure 6: Time evolution of water drop impacting on a moving hydrophobic wall (Teflon) obtained from 2D simulations. (a) $We_n = 39.8, We_t = 0.3$ (b) $We_n = 6.7, We_t = 5.5$ (c) $We_n = 42.3, We_t = 149$.

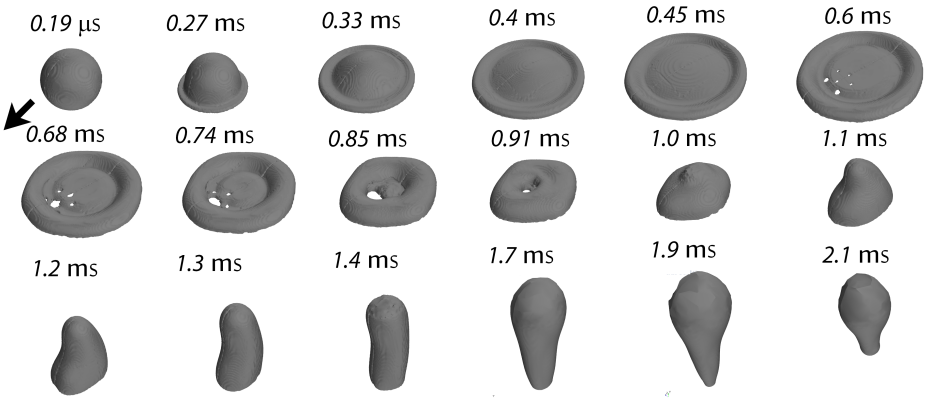

Figure 7: Time evolution of water drop impacting on a moving hydrophobic wall (Teflon) obtained from 3D simulations. This case corresponds to partial rebound in which $We_n = 39.8, We_t = 0.3$. Arrow denotes the surface motion direction.

on the surface. Unlike the first scenario, 2D simulations have shown similar behavior however for getting a physical insight we have considered the 3D results. Fig. 8a, 8b show the sequence of events happening for the case of deposition. As it is clear from the figure we cannot distinguish bubbles from the 3D reconstructed images, however side views of impact would reveal the bubble entrapment and motion of it till the extent that it escapes the liquid.

The third case ($We_n = 42.3, We_t = 149$) refers to the condition where split deposition happens in which the drop hits the moving wall, spreads over the surface but because of the high tangential velocity of the wall it splits and finally deposits on the surface. Results of 3D simulations corresponding to the case of split deposition is depicted in Fig. 9. In experimental results splitting happens at receding stage when the side which recedes in the opposite direction of the surface motion is hindered by the surface motion whereas on the other side receding flow is amplified because of motion in such a way that the connection between two sides gets thinner till it splits. But results of simulation shows at receding stage the entrapped bubble makes a bridge at the center and then gravity pulls down the top portion of liquid and drop deposits on the surface.

When we are dealing with drop impacts on moving surfaces, the drop is not spreading in circular shape because of the surface motion, instead it will spread in a tear-like shape. The ratio of the bigger diameter (b) to the smaller diameter (d_m) is represented by γ_A which is almost constant in two possible conditions as mentioned in [12]. In order to check the reliability of our results for the spreading process, this ratio was measured in our 3D simulations for deposition and partial rebound regimes (see Fig. 10).

4 Conclusion and Future Work

Simulations of drop impact on a hydrophobic moving surface have been done in both two and three dimensions. VOF model was used to capture the behavior of the interface. 2D simulations have predicted deposition and split deposition regimes correctly in terms of outcomes while they have shown a break up mainly because of the entrapped bubble at the stage of drop spreading in simulation of partial rebound regime. However, 3D simulations have shown that entrapped air did not cause breakup. 3D simulations captures the correct behavior in terms of outcome for deposition, while showing a total rebound instead of a partial rebound and deposition instead of split deposition. Receding stage is a period in which capillary forces and wettability play the most important role. Therefore, this discrepancy between 3D simulations and experiments might occur due to the use equilibrium contact angle for the whole duration of impact. In the future work, we will investigate the effect of dynamic contact angle to obtain results closer to experimental outcomes. Also, the effect of air boundary layer on the characteristics of drop impacts on moving surfaces can be another subject of future work.

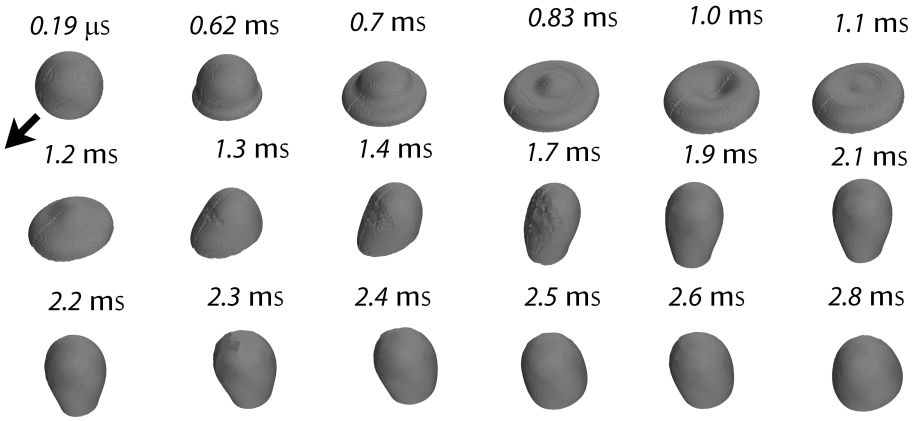

(a) 3D reconstructed deposition

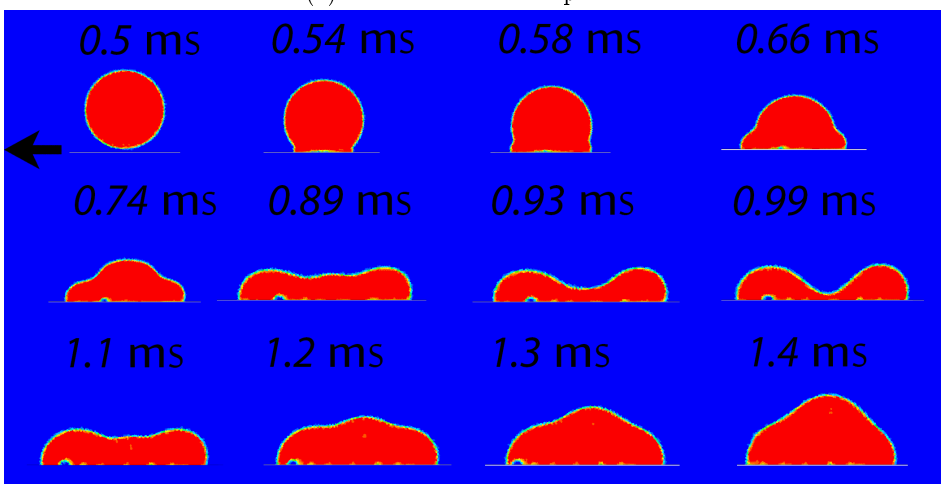

(b) Side view deposition

Figure 8: Time evolution of water drop impacting on a moving hydrophobic wall (Teflon) obtained from 3D simulations. This case corresponds to deposition in which $We_n = 6.7, We_t = 5.5$. Arrow denotes the surface motion direction. (a) 3D reconstructed version of deposition process (b) side view of deposition showing bubble escape (color codes denote the volume fraction and red denotes volume fraction of unity for water phase).

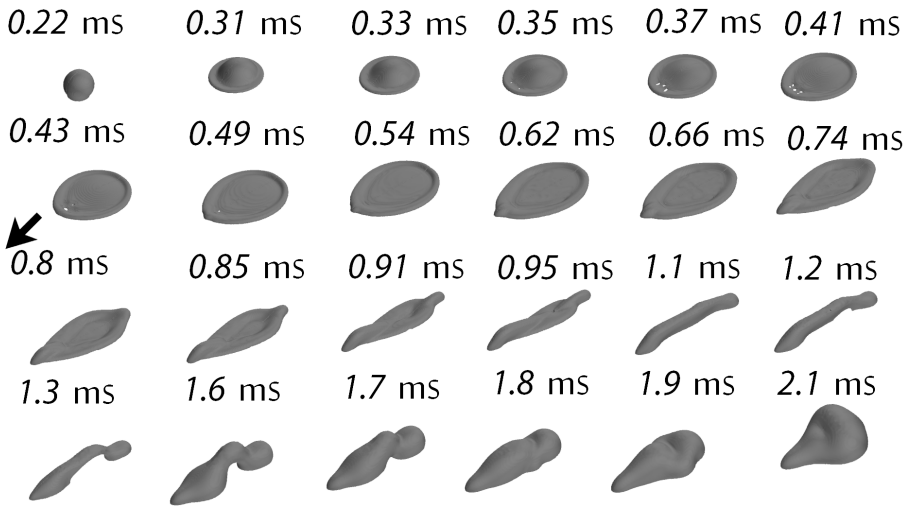

Figure 9: Time evolution of water drop impacting on a moving hydrophobic wall (Teflon) obtained from 3D simulations. This case corresponds to split deposition in which $We_n = 42.3, We_t = 149$. Arrow denotes the surface motion direction.

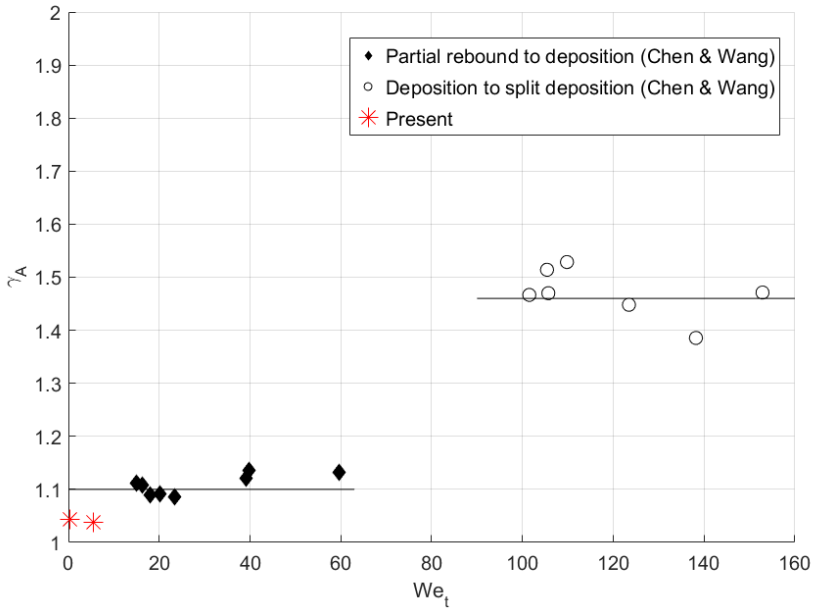

Figure 10: Ratio of diameters at maximum drop spreading. $\gamma_A = 1.1$ from the experimental data of [12] while it was 1.04 for deposition and partial rebound cases in our 3D simulations.

Acknowledgment

The authors would like to gratefully acknowledge Scientific and Technological Research Council of Turkey (TÜBİTAK) for providing financial support to this research with the 114M423 project. Also, authors thanks to to Asst. Prof. Dr. Ismail Arı for providing computational resources to carry out numerical simulations and Mr. Ayhan Sahin for the administration of the HPC servers.

References

[1] Arthur Mason Worthington. *A Study of Splashes*. Longmans, Green, and Company, 1908, 1908.

[2] Martin Rein. Phenomena of liquid drop impact on solid and liquid surfaces. *Fluid Dynamics Research*, 12(2):61–93, 2009.

[3] C. D. Stow and M. G. Hadfield. An Experimental Investigation of Fluid Flow Resulting from the Impact of a Water Drop with an Unyielding Dry Surface. *Proceedings of the Royal Society A: Mathematical, Physical and Engineering Sciences*, 373(1755):419–441, 1981.

[4] Chr. Mundo, M Sommerfeld, and C Tropea. Droplet-wall collisions: Experimental studies of the deformation and breakup process. *Int. J. Multiph. Flow*, 21(2):151–173, 1995.

[5] G E Cossali, A Coghe, and M Marengo. The impact of a single drop on a wetted solid surface, 1997.

[6] R Rioboo, Cam Tropea, and M Marengo. Outcomes from a drop impact on solid surfaces. *At. Sprays*, 11(2):155–165, 2001.

[7] R Rioboo, M Marengo, and C Tropea. Time evolution of liquid drop impact onto solid , dry surfaces. *Exp. Fluids*, 33:112–124, 2002.

[8] Guillaume Lagubeau, Marco a. Fontelos, Christophe Josserand, Agnès Maurel, Vincent Pagneux, and Philippe Petitjeans. Spreading dynamics of drop impacts. *Journal of Fluid Mechanics*, 713:50–60, oct 2012.

[9] a.L. Yarin. DROP IMPACT DYNAMICS: Splashing, Spreading, Receding, Bouncing.... *Annual Review of Fluid Mechanics*, 38(1):159–192, 2006.

[10] a Prosperetti. The Impact of Drops on Liquid Surfaces and the Underwater Noise of Rain. *Annual Review of Fluid Mechanics*, 25(1):577–602, 1993.

[11] James C. Bird, Scott S H Tsai, and Howard a. Stone. Inclined to splash: Triggering and inhibiting a splash with tangential velocity. *New Journal of Physics*, 11, 2009.

[12] R. H. Chen and H. W. Wang. Effects of tangential speed on low-normal-speed liquid drop impact on a non-wettable solid surface. *Experiments in Fluids*, 39:754–760, 2005.

[13] Saeed Fathi, Phill Dickens, and Farid Fouchal. Regimes of droplet train impact on a moving surface in an additive manufacturing process. *Journal of Materials Processing Technology*, 210:550–559, 2010.

[14] Tain Shi Zen, Fu Chu Chou, and Ju Lung Ma. Ethanol drop impact on an inclined moving surface. *Int. Commun. Heat Mass Transf.*, 37(8):1025–1030, 2010.

[15] James a. Sethian. Level Set Method and Fast Marching Mrthods. page 376, 1999.

[16] H. Bararnia, S.M. Seyyedi, D.D. Ganji, and B. Khorshidi. Numerical investigation of the coalescence and breakup of falling multi-droplets. *Colloids and Surfaces A: Physicochemical and Engineering Aspects*, 424:40–51, may 2013.

[17] Siddhartha F. Lunkad, Vivek V. Buwa, and K. D P Nigam. Numerical simulations of drop impact and spreading on horizontal and inclined surfaces. *Chemical Engineering Science*, 62(24):7214–7224, 2007.

[18] Metin Muradoglu and Savas Tasoglu. A front-tracking method for computational modeling of impact and spreading of viscous droplets on solid walls. *Computers and Fluids*, 39(4):615–625, 2010.

[19] G Tryggvason, B Bunner, A Esmaeeli, D Juric, N Al-Rawahi, W Tauber, J Han, S Nas, and Y J Jan. A front-tracking method for the computations of multiphase flow. *Journal of Computational Physics*, 169(2):708–759, 2001.

[20] Tuan Tran, Hélène de Maleprade, Chao Sun, and Detlef Lohse. Air entrainment during impact of droplets on liquid surfaces. *Journal of Fluid Mechanics*, 726:R3, 2013.

[21] S. T. Thoroddsen, T. G. Etoh, K. Takehara, N. Ootsuka, and Y. Hatsuki. The air bubble entrapped under a drop impacting on a solid surface. *Journal of Fluid Mechanics*, 545:203, 2005.

[22] V. Mehdi-Nejad, J. Mostaghimi, and S. Chandra. Air bubble entrapment under an impacting droplet. *Physics of Fluids*, 15(1):173–183, 2003.

[23] J. U. Brackbill, D. B. Kothe, and C. Zemach. A continuum method for modeling surface tension. *Journal of Computational Physics*, 100(2):335–354, 1992.